

# Gas-Phase Infrared Spectrum of the Protonated Water Dimer: Full-Dimensional (15D) Quantum-Dynamical Simulations

Oriol Vendrell,<sup>1</sup> Fabien Gatti,<sup>2</sup> and Hans-Dieter Meyer<sup>1,\*</sup>

<sup>1</sup>*Theoretische Chemie, Physikalisch-Chemisches Institut,*

*Universitaet Heidelberg, Im Neuenheimer Feld 229, 69120 Heidelberg, Germany*

<sup>2</sup>*LDSMS (UMR 536-CNRS), CC 014, Université de Montpellier II, F-34095 Montpellier, Cedex 05, France*

(Dated: January 17, 2007)

The infrared absorption spectrum of the protonated water dimer ( $\text{H}_5\text{O}_2^+$ ) is simulated in full dimensionality (15D) in the spectral range between 0 and 4000  $\text{cm}^{-1}$ . The calculations are performed using the Multiconfiguration Time-Dependent Hartree (MCTDH) method for propagation of wavepackets. The use of curvilinear coordinates is crucial for the adequate treatment of strong anharmonicities and large-amplitude torsions of the cation. An *exact* kinetic energy operator is used and the potential energy surface employed is that of Huang *et al.* [JCP,**122**,044308,(2005)]. Strong couplings between the proton-transfer and other modes are identified, and their role in the spectrum is discussed.

PACS numbers: 33.20.Ea, 02.70.Ns, 31.15.Qg

The dynamics and spectroscopy of water clusters [1, 2, 3] of different geometries as well as in bulk water [4] has attracted much research effort, mainly due to the major importance that proton transfer and general properties of water have in central areas of chemistry and biology. Accurate measurements of infrared (IR) spectra of small-size protonated water clusters have become possible in recent years [1, 2, 5, 6].

The protonated water dimer,  $\text{H}_5\text{O}_2^+$ , the smallest protonated water cluster, has been recently object of intense study. The infrared (IR) spectrum of the system has been measured in the gas phase, either using multiphoton dissociation techniques [1, 5] or measuring the vibrational predissociation spectrum of  $\text{H}_5\text{O}_2^+\cdot\text{RG}_n$  clusters with  $\text{RG}=\text{Ar,Ne}$  [2, 6]. The obtained spectra cannot be consistently assigned in terms of fundamental frequencies and overtones of harmonic vibrational modes due to the large-amplitude anharmonic motions and couplings of the cluster. Hence, more sophisticated theoretical approaches are required. Several theoretical studies have been conducted over the last years in order to understand and assign the IR spectrum of the cation [2, 7, 8, 9, 10, 11].

The first measurement [1] of the IR multiphoton dissociation spectrum (IRMPD) of  $\text{H}_5\text{O}_2^+$  spanned the range between 620 and 1900  $\text{cm}^{-1}$ . Three main absorptions were discussed and assigned, based on a previous quantum-dynamical simulation of the IR absorption spectrum on a 4D model of the hydrogen-bond (O-H-O) fragment [8]. Those assignments were revisited in the context of newer IRMPD experiments and calculations, producing somewhat disparate results [2, 5, 10, 11]. Recent measurements of the IR predissociation spectrum of the  $\text{H}_5\text{O}_2^+$  cation in argon-solvate [6] and neon- and argon-solvate [2] conditions present spectra with a simpler structure than the multiphoton IRMPD ones. It is expected that the spectrum of the  $\text{H}_5\text{O}_2^+\cdot\text{Ne}_1$  com-

plex is close to the linear absorption spectrum of the bare cation [2]. This spectrum features a doublet structure in the region of 1000  $\text{cm}^{-1}$  made of two well-defined absorptions at 928  $\text{cm}^{-1}$  and 1047  $\text{cm}^{-1}$ . This doublet structure has not yet been fully understood, although the highest-energy component has been already assigned to the asymmetric proton-stretch fundamental ([O-H-O<sub>||</sub>]) [2]. Another doublet structure appears in the experimental spectrum in the region 1800-1900  $\text{cm}^{-1}$ , that would be related to the water bending motions. At the same time, recent classical-dynamics simulations on accurate potential energy surfaces (PES) have shown that the [O-H-O<sub>||</sub>] motion features large amplitude displacements strongly coupled to other modes of the system. The central-proton displacement would then be involved in most of the lines appearing in the IR spectrum, since this motion relates to the largest changes in the dipole moment of the cation [10, 11]. Despite recent theoretical and experimental studies on this system, little is known about the lowest frequency region, between 0 and 900  $\text{cm}^{-1}$ . Modes vibrating in this frequency range are strongly anharmonic, and thus harmonic-vibrational analysis results are of little value in shedding light on that matter. These low frequency modes may play also an important role in combination with the [O-H-O<sub>||</sub>] fundamental. Such a possibility has been already suggested [5, 9, 10], but just which modes would participate in such combinations, and how, is still a matter of discussion.

In this letter we report the simulation of the IR linear absorption spectrum of the  $\text{H}_5\text{O}_2^+$  cation in the range between 0 to 4000  $\text{cm}^{-1}$  by means of a full-dimensional 15D quantum-dynamical treatment, using a set of curvilinear internal coordinates to tackle the anharmonicities and large-amplitude motions of the system. We also report the calculation of some fundamental frequencies and overtones, namely eigenenergies and eigenstates of the vibrational Hamiltonian, which are a key to the interpre-

tation and assignment of different spectral features. Our motivation is to illuminate the interpretation of the IR spectral signatures, which is still an open question. At the same time we want to stress that it is now possible, by state-of-the-art quantum-dynamical methods, to solve a 15D floppy and anharmonic molecular system with high accuracy, both in the time-dependent as well as in the time-independent representation. To address the problem, we make use of the potential energy surface (PES) and dipole-moment surfaces recently developed by Bowman and collaborators [7], which constitute the most accurate *ab initio* surfaces available to date for this system.

The quantum-dynamical problem is solved in the time-dependent picture using the multiconfiguration time dependent Hartree method (MCTDH)[12, 13]. MCTDH is an efficient algorithm to solve the time-dependent Schrödinger equation by means of a variationally optimal multiconfigurational expansion of the wavefunction. Each configuration is given by a Hartree-product of functions depending on a single or a group of degrees of freedom, the so-called single-particle functions (SPF). Both the multiconfigurational expansion coefficients and the SPF are allowed to vary simultaneously in time, which dramatically reduces the amount of configurations necessary to achieve a converged propagation as compared to the standard, numerically exact, propagation method. By controlling the number of configurations, MCTDH can be made as close to exact as desired, at the cost of an increased computational effort. The MCTDH program is also capable of using the time-independent picture, allowing for the convergence to eigenstates and eigenenergies of the Hamiltonian at hand. The algorithm that implements this feature is called *improved relaxation* [13, 14]. This algorithm is essentially a multiconfiguration self-consistent field approach that takes advantage of the MCTDH machinery. Several eigenenergies and eigenstates have been calculated using *improved relaxation*. They are invaluable in the assignments of some bands coming from the time-dependent calculation of the IR spectrum, and provide a total characterization of the corresponding states in terms of their fully-correlated wavefunctions. All the reported simulations were performed with the Heidelberg MCTDH package of programs [15].

The Hamiltonian is expressed in a set of polyspherical coordinates based on Jacobi vectors [16]. This set of coordinates allows for an adequate treatment of the anharmonic large-amplitude vibrations and torsions of the molecule. The kinetic energy operator is *exact* for  $J = 0$ , and the derivation of its lengthy formula (674 terms) will be discussed in a forthcoming publication. The correctness of the operator implemented was checked by comparison with data generated by the TNUM program [17]. The internal coordinates used are: the distance between the centers of mass of both water molecules ( $R$ ), the position of the central proton with respect to the center of mass of the water dimer ( $x, y, z$ ), the Euler angles defining

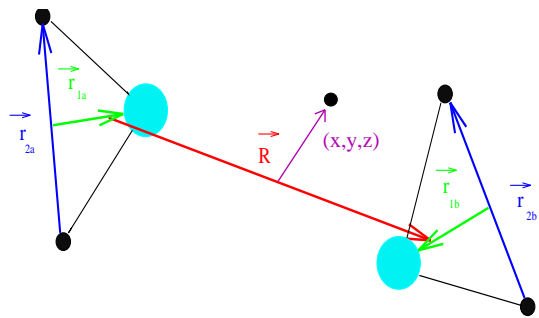


FIG. 1: (color online) Set of Jacobi vectors in terms of which the kinetic energy of the system is expressed. The set of internal coordinates used corresponds to the length of these vectors and relative angles.

the relative orientation between the two water molecules (wagging:  $\gamma_a, \gamma_b$ ; rockings:  $\beta_a, \beta_b$ ; internal relative rotation:  $\alpha$ ) and the Jacobi coordinates which account for the particular configuration of each water molecule ( $r_{1(a,b)}, r_{2(a,b)}, \theta_{(a,b)}$ ) where  $r_{1x}$  is the distance between the oxygen atom and the center of mass of the corresponding  $H_2$  fragment,  $r_{2x}$  is the H–H distance and  $\theta_x$  is the angle between these two vectors. These coordinates have the great advantage of leading to a much more decoupled representation of the PES than a normal-mode based Hamiltonian.

As outlined above, the wavefunction is represented by products of SPFs which in turn are represented by discrete variable representation (DVR) grids. The total primitive product-grid consists of  $1.3 \times 10^{15}$  points. This number makes clear that the potential must be represented in a more compact form to make calculations feasible. We choose to represent the PES as follows: the coordinates are divided in five groups,  $\mathbf{g}_1 \equiv [x, y, z, \alpha]$ ,  $\mathbf{g}_2 \equiv [\gamma_a, \gamma_b]$ ,  $\mathbf{g}_3 \equiv [R, \beta_a, \beta_b]$ ,  $\mathbf{g}_4 \equiv [r_{1a}, r_{2a}, \theta_a]$  and  $\mathbf{g}_5 \equiv [r_{1b}, r_{2b}, \theta_b]$ . The potential is then expanded as [18]:

$$\hat{V}(\mathbf{c}) = \hat{v}^{(0)} + \sum_{i=1}^5 \hat{v}_i^{(1)}(\mathbf{g}_i) + \sum_{i=1}^4 \sum_{j=i+1}^5 \hat{v}_{ij}^{(2)}(\mathbf{g}_i, \mathbf{g}_j) + \hat{v}_{z,2,3}^{(3)}(z, \mathbf{g}_2, \mathbf{g}_3) \quad (1)$$

where  $\mathbf{c} \equiv [\mathbf{g}_1, \dots, \mathbf{g}_5]$ . The  $\hat{v}^{(0)}$  term is the energy at the reference geometry. The  $\hat{v}_i^{(1)}$  terms are the intra-group potentials obtained by keeping the coordinates in other groups at the reference geometry, while the  $\hat{v}_{ij}^{(2)}$  terms account for the group-group correlations. The potential with up to second-order terms gives already a very reasonable description of the system. The  $\hat{v}_{z,2,3}^{(3)}$  term accounts for three-mode correlations between the displacement of the central proton, the distance between both water molecules and the angular wagging and rocking motions. This PES representation may be sequentially

improved in a convergent series by adding more correction terms where coordinates belonging to three or more different groups are allowed to vary simultaneously. However, the PES in Eq. 1 is found to reproduce the full potential very well, providing a converged zero-point energy of  $12376.3 \text{ cm}^{-1}$ ,  $16 \text{ cm}^{-1}$  below the reported Diffusion-Monte-Carlo result [19] on the full potential.

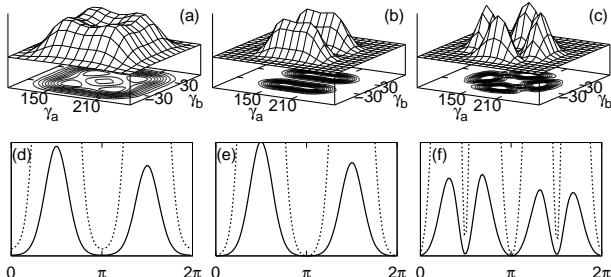


FIG. 2: Probability density of the ground vibrational state (a), first (b) and third (c) wagging-mode states projected onto the wagging coordinates  $\gamma_a$  and  $\gamma_b$ . Ground vibrational state (d), splitting state (e) and second excited internal-rotation state (f) projected onto the  $\alpha$  coordinate. An extended scale ( $\times 10$ ) is used to clarify existence and position of nodes.

In Fig. 2 the probability-density projection on the wagging coordinates is shown for the ground vibrational state ( $g_0$ ), as well as for one of the two fundamental states ( $w_{1a}, w_{1b}$ ) of the wagging modes, which are degenerate vibrational states with an energy of  $106 \text{ cm}^{-1}$ . The energies of the next three wagging-mode states ( $w_2, w_3, w_4$ ) are, respectively,  $232$ ,  $374$  and  $422 \text{ cm}^{-1}$ . State  $w_2$  has an energy that nearly doubles the energy of the  $w_{1x}$  states, since it has been seen to roughly correspond to one quantum in state  $w_{1a}$  and one quantum in state  $w_{1b}$ . The strong anharmonicity of the wagging motions can be further appreciated in the progression of  $w_2$ ,  $w_3$  and  $w_4$  vibrational-state energies. In addition, the harmonic-analysis energies of the two lowest wagging-fundamentals  $w_{1a}$  and  $w_{1b}$  are around  $300 \text{ cm}^{-1}$  larger than the MCTDH result and do not account for their degeneracy, since harmonic modes are constructed taking as a reference the  $C_{2v}$  absolute minimum. The system, however, interconverts between equivalent  $C_{2v}$  minima and other stationary points through low-energy barriers (wagging motions and internal rotation), which leads to a highly symmetric ground-state wavefunction. The vibrational levels of  $\text{H}_5\text{O}_2^+$  can be labeled according to the symmetry group  $\mathcal{G}_{16}$ , which is related to the  $\mathcal{D}_{2d}$  point group but with allowed permutation of the H-atoms within each of the two monomers [20]. The two lowest excited wagging/rocking modes transform according to an  $E$  representation within this symmetry group.

The first two excited states associated to the internal rotation ( $g_0^{(-)}$ ,  $i_1$ ) have energies of  $1$  and  $160 \text{ cm}^{-1}$ , respectively. Here  $g_0^{(-)}$  is the splitting state whose proba-

bility density along  $\alpha$  is shown in Fig. 2e, while the probability density for  $i_1$  is shown in Fig. 2f. The first two fundamentals of the symmetric stretch ( $[\text{O-O}]_{\parallel}$ ,  $R$  coordinate) have energies of  $550$  and  $1069 \text{ cm}^{-1}$  respectively, while the rocking fundamentals, which are degenerate, have an energy of  $456 \text{ cm}^{-1}$ .

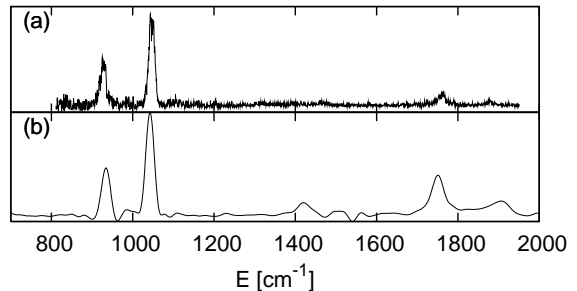


FIG. 3: Predissociation spectrum of the  $\text{H}_5\text{O}_2^+\cdot\text{Ne}$  complex [3] (top) and MCTDH (bottom).

Figure 3 presents the IR predissociation spectrum of the  $\text{H}_5\text{O}_2^+\cdot\text{Ne}$  complex [2] and the MCTDH spectrum of  $\text{H}_5\text{O}_2^+$  in the range  $700$ - $1900 \text{ cm}^{-1}$ . The MCTDH spectrum is obtained in the time-dependent picture by Fourier transformation of the autocorrelation of the dipole-operated initial state [21]:

$$I(E) = \frac{E}{6 c \epsilon_0 \hbar^2} \int_{-\infty}^{\infty} \exp(i(E + E_0)t/\hbar) \times \langle \Psi_{\mu,0} | \exp(-i\hat{H}t/\hbar) | \Psi_{\mu,0} \rangle dt \quad (2)$$

where  $E_0$  is the ground-state energy and  $|\Psi_{\mu,0}\rangle \equiv \hat{\mu} |\Psi_0\rangle$ . The MCTDH spectrum shows a good agreement with the experimental spectrum. The agreement on the doublet structure around  $1000 \text{ cm}^{-1}$  is very good, and the position of the doublet at  $1700$  -  $1800 \text{ cm}^{-1}$  is also in good agreement, despite the relative intensities being larger in MCTDH. The doublet absorption at around  $1000 \text{ cm}^{-1}$  deserves a deeper analysis. Due to the high density of states, it was not possible, by means of *improved relaxation*, to obtain the fully converged states, but reasonably good approximations to the wavefunctions of the low-energy ( $|\Psi_d^l\rangle$ ,  $930 \text{ cm}^{-1}$ ) and high energy ( $|\Psi_d^h\rangle$ ,  $1021 \text{ cm}^{-1}$ ) eigenstates of the doublet were computed. Even though these wavefunctions contain all the possible information on the two states, their direct analysis becomes complex due to the high dimensionality of such objects. In order to obtain a fundamental understanding of the observed bands, zeroth-order, i. e. Hartree, states are constructed by diagonalization of 1-mode Hamiltonian operators, where the modes are those defined around Eq. 1. The two eigenstates corresponding to the doublet are then projected onto the zeroth-order states. Two of them are found to play a major role:  $|\Phi_z\rangle$ , with one quantum of excitation in the proton-transfer coordinate, and  $|\Phi_{R,w_3}\rangle$ , with one quantum in  $[\text{O-O}]_{\parallel}$  and

three quanta in the wagging motion. The corresponding overlaps read:  $|\langle\Phi_z|\Psi_d^l\rangle|^2 = 0.12$ ,  $|\langle\Phi_{R,w_3}|\Psi_d^l\rangle|^2 = 0.44$  and  $|\langle\Phi_z|\Psi_d^h\rangle|^2 = 0.23$ ,  $|\langle\Phi_{R,w_3}|\Psi_d^h\rangle|^2 = 0.04$ . The overlaps with other Hartree states are much smaller. One should take into account that these numbers depend on the exact definition of the zeroth-order states, which is not unique. Also, the zeroth-order states do not span the same space as the two eigenstates, so the overlaps do not add up to 1. However, they provide a clear picture of the nature of the doublet: the low-energy band has the largest contribution from the combination of the symmetric stretch and the third excited wagging (see Fig. 2), whereas the second largest is the proton-transfer motion. For the high-energy band the importance of these two contributions is reversed. Thus, the doublet may be regarded as a Fermi resonance between two zero-order states which are characterized by  $(1R, 3w)$  and  $(1z)$  excitations, respectively. The reason why the third wagging excitation plays an important role in the proton-transfer doublet is understood by inspecting Fig. 2c. The probability density of this state has four maxima, each of which corresponds to a planar conformation of  $\text{H}_2\text{O}-\text{H}^+$  ( $\text{H}_3\text{O}^+$  character) for one of the waters, and a bend conformation ( $\text{H}_2\text{O}$  character) where a lone-pair  $\text{H}_2\text{O}$  orbital forms a hydrogen bond with the central proton. When the proton oscillates between the two waters, the two conformations exchange their characters accordingly.

The simulated spectrum in the range between 0 and  $4000\text{ cm}^{-1}$  is depicted in Fig. 4. The region below  $700\text{ cm}^{-1}$  has not yet been accessed experimentally. Direct absorption of the wagging motions, excited by the  $x$  and  $y$  components of the dipole operator, appears in the range between  $100 - 200\text{ cm}^{-1}$ . The doublet starting at  $1700\text{ cm}^{-1}$  is clearly related to bending motions of the water molecules, but its exact nature is still to be addressed. The MCTDH spectrum also shows the absorptions of the OH stretchings starting at  $3600\text{ cm}^{-1}$ .

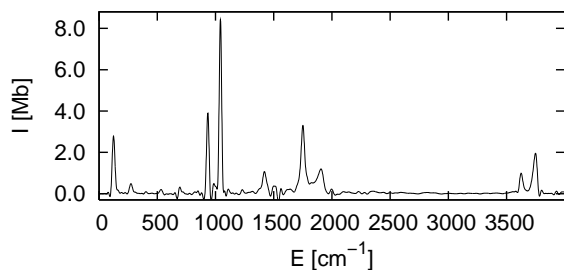


FIG. 4: Simulated MCTDH spectrum in the range between 0 and  $4000\text{ cm}^{-1}$ . Absorption is given in absolute scale in mega-barns (Mb).

To summarize, in this work we report the simulation of

the IR absorption spectrum of the  $\text{H}_5\text{O}_2^+$  cation by means of the quantum-dynamical MCTDH method, using an exact kinetic-energy operator and an accurate potential energy surface. The use of curvilinear coordinates was essential because only then the strongly anharmonic large-amplitude motions (wagging, torsion, rockings) could be described conveniently. The reported simulations show a good agreement with the predissociation spectrum of the  $\text{H}_5\text{O}_2^+\cdot\text{Ne}$  complex. Moreover, they clarify various features of the IR spectrum that remained elusive due to complicated anharmonicities and couplings.

The authors thank Prof. J. Bowman for providing the potential-energy routine, D. Lauvergnat for performing the TNUM calculations and the Scientific Supercomputing Center Karlsruhe for generously providing computer time. O. V. is grateful to the Alexander von Humboldt Foundation for financial support.

---

\* Hans-Dieter.Meyer@pci.uni-heidelberg.de

- [1] K. R. Asmis, *et al.*, *Science* **299**, 1375 (2003).
- [2] N. I. Hammer, *et al.*, *J. Chem. Phys.* **122**, 244301 (2005).
- [3] J. M. Headrick, *et al.*, *Science* **308**, 1765 (2005).
- [4] D. Marx, M. Tuckerman, J. Hutter, and M. Parrinello, *Nature* **397**, 601 (1999).
- [5] T. D. Fridgen, *et al.*, *J. Phys. Chem. A* **108**, 9008 (2004).
- [6] J. M. Headrick, J. C. Bopp, and M. A. Johnson, *J. Chem. Phys.* **121**, 11523 (2004).
- [7] X. Huang, B. J. Braams, and J. M. Bowman, *J. Chem. Phys.* **122**, 044308 (2005).
- [8] M. V. Vener, O. Kühn, and J. Sauer, *J. Chem. Phys.* **114**, 240 (2001).
- [9] J. Dai, *et al.*, *J. Chem. Phys.* **119**, 6571 (2003).
- [10] J. Sauer and J. Dobler, *Chem. Phys. Chem.* **6**, 1706 (2005).
- [11] M. Kaledin, A. L. Kaledin, and J. M. Bowman, *J. Phys. Chem. A* **110**, 2933 (2006).
- [12] M. H. Beck, A. Jäckle, G. A. Worth, and H.-D. Meyer, *Phys. Rep.* **324**, 1 (2000).
- [13] H.-D. Meyer and G. A. Worth, *Theor. Chem. Acc.* **109**, 251 (2003).
- [14] H.-D. Meyer, F. Le Quéré, C. Léonard, and F. Gatti, *Chem. Phys.* **329**, 179 (2006).
- [15] G. A. Worth, M. H. Beck, A. Jäckle, and H.-D. Meyer, *The MCTDH Package, Version 8.4*, (2007). See <http://www.pci.uni-heidelberg.de/tc/usr/mctdh/>.
- [16] F. Gatti, *J. Chem. Phys.* **111**, 7225 (1999).
- [17] D. Lauvergnat and A. Nauts, *J. Chem. Phys.* **116**, 8560 (2002).
- [18] J. M. Bowman, S. Carter, and X. Huang, *Int. Rev. Phys. Chem.* **22**, 533 (2003).
- [19] A. B. McCoy, *et al.*, *J. Chem. Phys.* **122**, 061101 (2005).
- [20] D. J. Wales, *J. Chem. Phys.* **110**, 10403 (1999).
- [21] G. G. Balint-Kurti, R. N. Dixon, and C. C. Marston, *J. Chem. Soc., Faraday Trans.* **86**, 1741 (1990).